CONFINEMENT REINFORCEMENT DESIGN CONSIDERATIONS FOR DUCTILE HSC COLUMNS

By Oguzhan Bayrak[1] and Shamim A. Sheikh[2]

ABSTRACT: This paper presents results from a continuing research program that aims to study confinement of concrete by lateral reinforcement. The current work deals with the experimental behavior of high-strength concrete (HSC) and ultrahigh-strength concrete (UHSC) column behavior. Realistically sized columns (305 × 305 × 1,473 mm) with heavy stubs (508 × 762 × 813 mm) were tested under moderate to high axial load levels and reversed cyclic displacement excursions. The behavior of UHSC and HSC columns were examined and compared to normal strength concrete column behavior. The variables studied in this research program are the concrete strength, axial load level, steel configuration, amount of lateral steel, and the presence of a heavy stub. A performance-based design procedure for the design of confinement reinforcement in HSC and UHSC columns is presented and compared with current American Construction Institute (United States) and New Zealand Standards (New Zealand) codes.

INTRODUCTION

According to current seismic design philosophy, the ability of concrete-framed structures to withstand strong ground motions depends mainly on the formation of plastic hinges and their capacities to absorb and dissipate energy without significant loss of strength. For this reason, most building codes attempt to ensure hinging in the beams rather than the columns to guarantee stability. However, recent earthquakes and analytical investigations (Paulay 1977; Mitchell and Paultre 1994; Bayrak 1995) show that formation of plastic hinges in columns of a framed structure, at locations other than the column bases at the foundation level, is still possible as a result of a severe earthquake despite the application of the "strong column-weak beam" concept, as recommended by various design codes. During the last two decades, the use of high-strength concrete (HSC) has become widespread adding another dimension to the design problem. The equations that exist in the current design codes [ACI 318-95 ("Building" 1995), CAN3-A23.3-M94 ("Code" 1994), and NZS3101:1995 ("Code" 1995a,b)] were originally derived based on experimental results in which normal strength concrete (NSC) was used. Therefore the applicability of current code provisions for the design of confinement reinforcement in HSC columns and for the calculation of moment capacity of HSC column sections has to be investigated.

The work presented here, is part of a comprehensive research program (Sheikh and Uzumeri 1980; Sheikh and Khoury 1993; Sheikh and Toklucu 1993; Bayrak and Sheikh 1996) that aims to study confinement of concrete by circular as well as rectilinear lateral reinforcement. The current work deals with the experimental behavior of concrete columns confined by rectilinear ties and subjected to moderate to high levels of axial load and cyclic lateral displacements simulating earthquake effects. The main focus of the current work is on the earthquake performance of ultrahigh-strength concrete (UHSC) specimens with concrete strength of 102 MPa. UHSC specimen behavior is compared with HSC specimen behavior (Bayrak and Sheikh 1996) and NSC specimen behavior (Sheikh and Khoury 1993). This comparison allows a direct evaluation of the effect of concrete strength. The effects of reinforcement configuration, amount of lateral reinforcement, and axial load level on the behavior of columns are also evaluated. The validity of a recently proposed performance-based confinement reinforcement design procedure (Sheikh and Khoury 1997) for NSC columns is checked against HSC and UHSC test data. To make these design equations applicable to HSC and UHSC columns, a modification to this design procedure is suggested. The suggested procedure is compared with NZS 3101:1995 code's requirements which essentially have a very similar form with the design equations derived by Watson et al. (1994) and Watson and Park (1994).

RESEARCH SIGNIFICANCE

In most concrete design codes (ACI 318-95, CAN3-A23.3-M94, and NZS3101:1995) provisions for the design of confinement reinforcement and calculation of moment capacity contain empirical constants. In the derivation of these empirical constants experimental data available in the literature were used. The majority of the data utilized was from tests in which NSC was used. Only recently, a very limited amount of experimental data on HSC columns has become available. Experimental data on UHSC column behavior can rarely be found in the literature, especially on realistically sized columns tested under moderate to high axial load levels and subjected to large inelastic displacement excursions.

Design engineers have no option but to use the equations provided in concrete design codes. There is still a lot to be known about HSC and UHSC column behavior; due to their appealing mechanical properties HSC and UHSC are being used regularly by design engineers. This necessitates the evaluation of applicability of relevant requirements of concrete design codes to HSC and UHSC and is partially accomplished using the experimental data obtained from this research.

A more rational design procedure for the design of confinement reinforcement in normal strength columns has been suggested by Khoury and Sheikh (1991) and Sheikh and Khoury (1997). Concrete strengths up to 55 MPa were used in the experimental work upon which the design equations were based. Test data on HSC and UHSC column behavior from this research are used to evaluate the validity of the suggested design procedure and necessary modifications are suggested. Watson et al. (1994) reported another rational design procedure that forms the basis of the current New Zealand code's requirement. These equations were mainly based on experimental data reported by Watson and Park (1994). All of the 11 columns reported in Watson and Park's paper were made of concrete with strengths ranging from 39 to 47 MPa.

[1]PhD Candidate, Dept. of Civ. Engrg., Univ. of Toronto, Toronto, Ontario, M5S 1A4, Canada.

[2]Prof., Dept. of Civ. Engrg., Univ. of Toronto, Toronto, Ontario, M5S 1A4, Canada.

Note. Associate Editor: Walter H. Gerstle. Discussion open until February 1, 1999. To extend the closing date one month, a written request must be filed with the ASCE Manager of Journals. The manuscript for this paper was submitted for review and possible publication on November 21, 1996. This paper is part of the ***Journal of Structural Engineering***, Vol. 124, No. 9, September, 1998. ©ASCE, ISSN 0733-9445/98/0009-0999–1010/$8.00 + $.50 per page. Paper No. 14626.

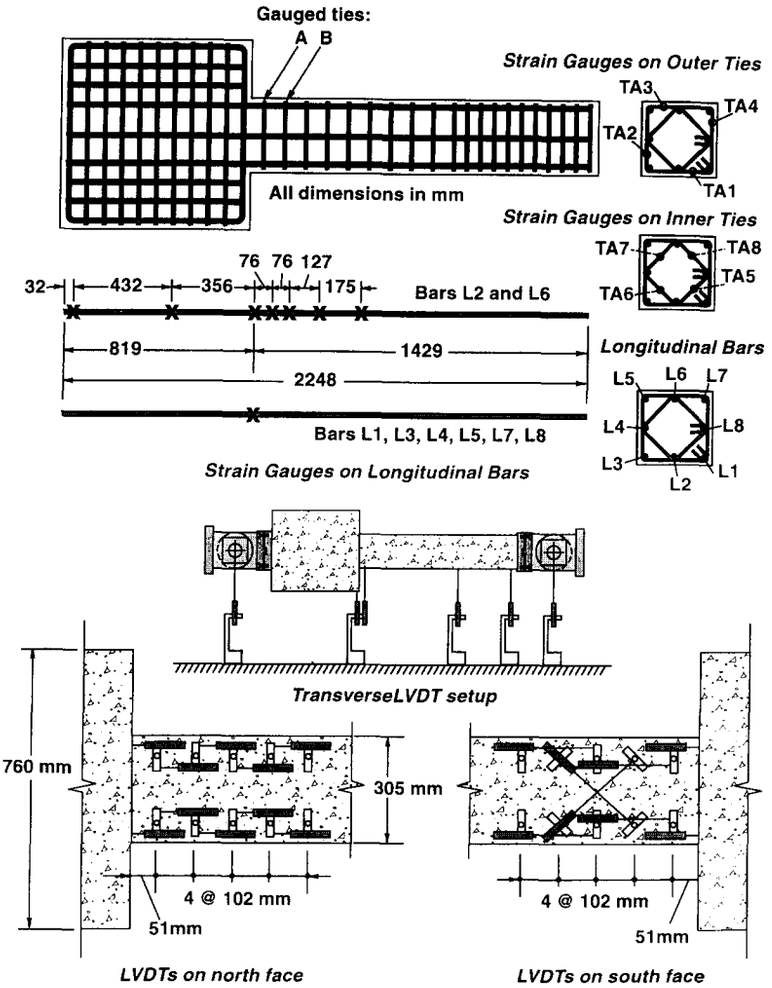

FIG. 1. Location of Strain Gauges and LVDTs

TABLE 1. Member and Section Ductility Parameters

			Lateral Reinforcement				Axial Load		Ductility Factor			Ductility Ratios				Energy Indicators			
Specimen (1)	$R_{M/P}$ (2)	f'_c (MPa) (3)	Size @ spacing (mm) (4)	ρ_s (%) (5)	f_{yh} (MPa) (6)	$\frac{A_{sh}}{A_{sh(ACI)}}$ (7)	$\frac{P}{f'_c A_g}$ (8)	$\frac{P}{P_0}$ (9)	μ_Δ at $0.8P_{max}$ (10)	μ_ϕ at $0.8M_{max}$ (11)	μ_ϕ at $0.9M_{max}$ (12)	$N_{\Delta 80}$ (13)	$N_{\Delta t}$ (14)	$N_{\phi 80}$ (15)	$N_{\phi t}$ (16)	W_{80} (17)	W_t (18)	E_{80} (19)	E_t (20)
AS-5HT	2.3	101.8	10M @ 90	4.02	542.0	1.09	0.45	0.48	4.0	9.6	5.6	14	35	27	49	23	98	144	311
	2.3	101.8	15M @ 90	4.02	463.0	1.09	0.45	0.48	4.0	9.6	5.6	14	35	27	49	23	98	144	311
AS-6HT	3.5	101.9	15M @ 76	6.74	463.0	1.70	0.46	0.49	6.3	14.0	10.4	23	68	54	114	49	230	450	1,243
AS-7HT	1.7	102.0	10M @ 94	2.72	542.0	0.80	0.45	0.48	3.1	7.2	5.5	9	12	14	24	11	17	25	57
ES-8HT	2.2	102.2	15M @ 70	4.29	463.0	1.08	0.47	0.50	3.6	6.7	5.1	11	16	14	22	18	32	33	99
ES-1HT	2.3	72.1	15M @ 95	3.15	463.0	1.13	0.50	0.50	4.6	6.6	5.9	15	20	19	25	33	57	80	105
AS-2HT	3.3	71.7	10M @ 90	2.84	542.0	1.19	0.36	0.36	6.2	15.8	13.6	18	61	53	113	41	313	631	1,412
AS-3HT	2.4	71.8	10M @ 90	2.84	542.0	1.19	0.50	0.50	5.0	10.1	9.1	15	28	20	42	36	102	161	396
AS-4HT	3.7	71.9	15M @ 100	5.12	463.0	1.83	0.50	0.50	7.0	21.2	17.7	25	69	84	151	231	354	997	1,688

EXPERIMENTAL PROGRAM

Results from the tests of four large-scale UHSC column specimens made from 102-MPa concrete are presented. All of the column-stub specimens were tested under constant moderate to high axial loads and large cyclic inelastic displacements. These results are compared with results from recent tests (Bayrak and Sheikh 1996) on HSC concrete specimens made of 72-MPa concrete and earlier tests (Sheikh and Khoury 1993; Sheikh et al. 1994) on similar specimens having concrete strengths between 30 and 55 MPa.

The level of axial load, as measured by the index P/P_0, was roughly equal to 0.50 for all of the currently tested UHSC specimens. On the other hand, for recently tested HSC column specimens P/P_0 varied between 0.36 and 0.50 to evaluate the effect of axial load on HSC specimen behavior. Test specimens were subjected to considerably high axial loads because most of the concrete design codes allow high axial loads. Only a very limited amount of test data are available for large-size UHSC specimens tested under these levels of axial load, especially when they are subjected to very large inelastic displacement cycles.

Specimens

Specimens consisted of 305 × 305 × 1,473 mm columns cast integrally with 508 × 762 × 813 mm stubs (Fig. 1). The column part of the specimen represents the part of a column

in a regular building frame between the section of maximum moment and the point of contraflexure. The stub represents a discontinuity like a beam-column joint or a footing adjacent to the section of maximum moment. Table 1 includes details of the test specimens.

Concrete and Reinforcement

Ready-mix normal weight concrete was used. The concrete strength of each specimen (Table 1) was obtained by averaging three standard cylinder tests' results. Three different types of reinforcing bars were used to construct specimens. 10M (100 mm^2) and 15M (200 mm^2) bars were used for the ties and 20M (300 mm^2) size was used for the longitudinal bars. Stress-strain curves of steel in tension are given in Fig. 2. Each curve represents an average of three test results.

Reinforcing Cages

The reinforcement for the stub consisted of 10M (100 mm^2) lateral and longitudinal stirrups at 64 mm spacing. The longitudinal bars in columns were extended through the stub to 20 mm from the ends in all specimens. The ties were placed at predetermined spacing within the 910-mm-long test regions of the columns adjacent to the stubs. Beyond that point, the spacing was reduced to half of the predetermined value to provide extra confinement and to reduce chances of failure. This was an extra precaution, and in none of the tests were the stresses outside the test region close to being critical. No cracks were observed outside of the test region, meaning strains were very small and confinement steel was not effective. Two different reinforcement configurations (Fig. 1) were used in the test regions of the columns. Minimum anchorage of ties conformed to the ACI building code's requirements (1995). No anchorage failure was observed in any specimen.

Instrumentation

Concrete and reinforcement strains at various locations, deflections along the specimen length, and axial and lateral loads were monitored during each test through the use of extensive instrumentation. Fig. 1 shows the locations of strain gauges on longitudinal and lateral reinforcement, as well as the linear variable differential transducer (LVDT) arrangement. Two sets of ties in the column closest to the stub were instrumented with strain gauges. Longitudinal concrete strains in the core were measured by using LVDTs over gauge lengths that ranged from 51 to 102 mm and covered a length of ~460 mm from the column-stub interface. Longitudinal strains at the top and bottom of the concrete core were monitored in a segmental form to locate the section showing the largest deformations. The first segment from the stub's face was 51 mm wide and the subsequent four segments were 102 mm wide (Fig. 1). Lateral deflections at six locations along the length of the specimens were measured using LVDTs. Shear deformations in the plastic hinge region were also measured through the use of two diagonally placed LVDTs. In each test, a total of 24 LVDTs were used to monitor axial as well as transverse deformations.

Testing

All of the specimens were tested under constant axial load and reversed cyclic displacement excursions in the test frame illustrated in Fig. 3. A 4,450-kN hydraulic jack and a load cell of similar capacity were used to apply and measure the axial load. Optical measurement devices were used for the alignment of the specimen. To check the alignment, axial load was applied in 250-kN intervals and the strain gauges and LVDTs were monitored regularly. In most specimens, very little adjustment was required, but when necessary the specimen was unloaded for adjustment. After the final positioning, the alignment was checked to the maximum predetermined axial load, and the lateral load actuator was connected to the specimen after applying the full axial load. The specimen was then subjected to predetermined displacement excursions (Fig. 4). All specimens were first loaded downward (with respect to the test frame shown in Fig. 3). In the first cycle the specimen was subjected to 75% of the elastic or yield displacement Δ_1, which can be defined as the lateral deflection corresponding to the estimated lateral load-carrying capacity (V_{max}) on a straight line joining origin and a point ~65% of V_{max} on the lateral load-displacement curve (Fig. 5). In all the test specimens the ascending parts of the lateral load-displacement envelopes were linear up to at least 70% of the maximum lateral load, and hence the method used was essentially the initial tangent approach. It should be recognized that both Δ_1 and V_{max} were calculated using the theoretical sectional response of the unconfined column and integrating curvatures along the length of the specimen. Moment generated by the axial load was not considered in the calculation of Δ_1 since this effect is minimal in the earlier stages of column response. The specimen was subjected to increasing reversed cyclic displacement excursions until it was unable to maintain the originally applied axial load.

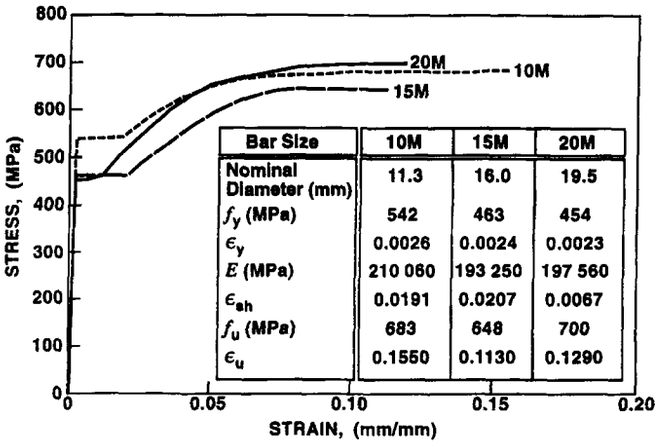

Bar Size	10M	15M	20M
Nominal Diameter (mm)	11.3	16.0	19.5
f_y (MPa)	542	463	454
ϵ_y	0.0026	0.0024	0.0023
E (MPa)	210 060	193 250	197 560
ϵ_{sh}	0.0191	0.0207	0.0067
f_u (MPa)	683	648	700
ϵ_u	0.1550	0.1130	0.1290

FIG. 2. Stress-Strain Behavior of Steel

TEST RESULTS

Behavior of each specimen is presented graphically in the form of column shear force-versus-tip deflection and moment-versus-curvature relationships. Fig. 6 shows the idealization of a specimen and the definitions of shear force V and tip deflection Δ_t used in Figs. 7–14. The deflection at the failed section was determined from the measured deflected shape of the column and was used to calculate secondary moment due to axial load. The moments plotted in Figs. 7–14 are those at the failed sections of the columns, and they include secondary moments caused by the axial load. The curvature was calculated from the deformation readings measured by the upper and lower LVDTs located in the most damaged region within the hinging zone. The gauge lengths were kept constant in all the specimens. Spalling of top and bottom concrete covers, yielding of inner and outer ties, and buckling of top and bottom longitudinal bars are marked on the graphs in Figs. 7–10. In all of the specimens failure did not occur at the column-stub connection, although this section was subjected to the maximum moment. Due to the additional confinement provided by the stub to the adjacent column section, the failure shifted away from the stub.

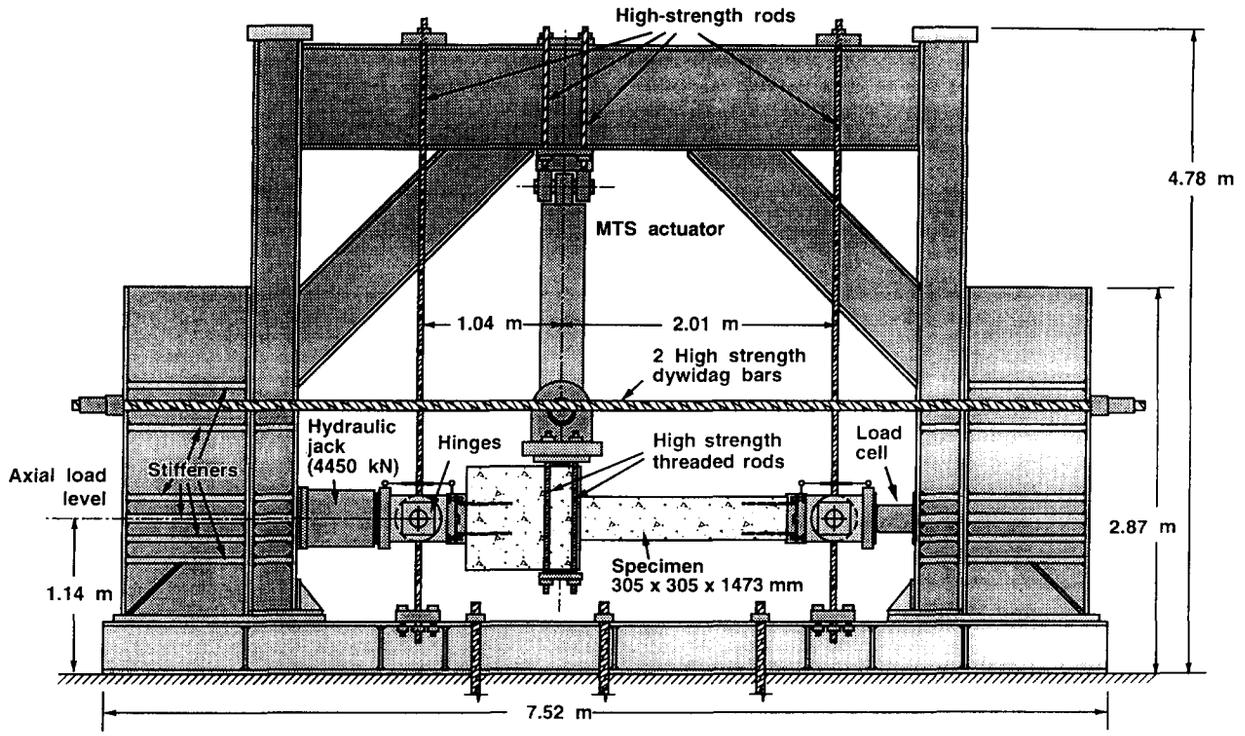

FIG. 3. Schematic of Test Setup

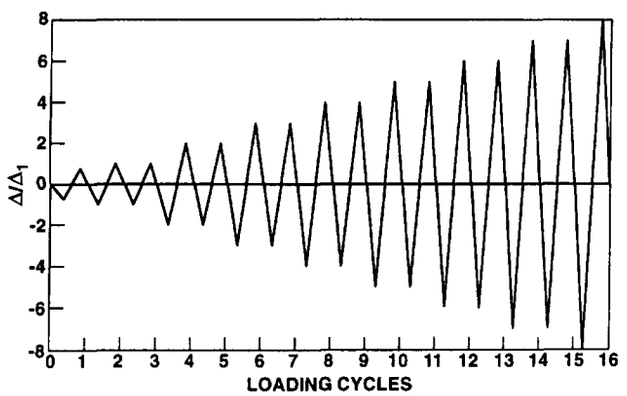

FIG. 4. Specified Displacement History

Test Observations

As in NSC and HSC specimens, the first signs of distress in all of the tested specimens were the cracks in the top and bottom concrete covers. On the other hand, the number of cracks formed in the first three cycles seemed to be slightly lower than those in the HSC specimens. In HSC specimens having a concrete strength of 72 MPa, the average distance between flexural cracks ranged between 60 and 100 mm. In UHSC specimens this spacing varied between 80 and 140 mm. For Specimens AS-5HT, AS-6HT, and AS-7HT top concrete spalled off suddenly just before the first downward peak of the fourth cycle ($\Delta = 2\Delta_1$), and the bottom concrete spalled off at the upward (with respect to the test frame shown in Fig. 3) peak of the same cycle. For Specimen ES-8HT, top concrete spalled off at the first peak of the fourth cycle ($\Delta = 2\Delta_1$), and the bottom concrete severely cracked at the upward peak of the same cycle and spalled off in the next cycle. The concrete strain at the time of spalling of cover concrete was 0.0029, 0.0027, 0.0030, and 0.0029 for Specimens AS-5HT, AS-6HT, AS-7HT, and ES-8HT, respectively. After the sixth cycle ($\Delta = 3\Delta_1$), cracking propagated to the sides of the column followed by cover spalling at the sides of the specimen. Lateral flexural cracks formed first in the hinging zone at a distance of ~175–300 mm from the face of the stub and extended further in later stages toward the stub. The most extensive damage was concentrated at ~200–300 mm from the face of the stub and extended toward the stub in later stages. Spalling of the

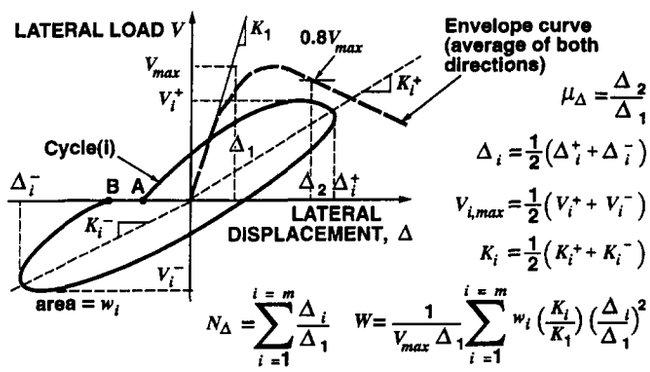

(a) Member Ductility Parameters

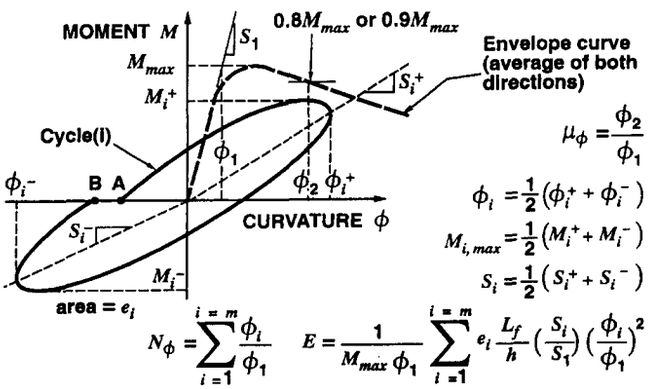

(b) Section Ductility Parameters

FIG. 5. Definitions of Ductility Parameters

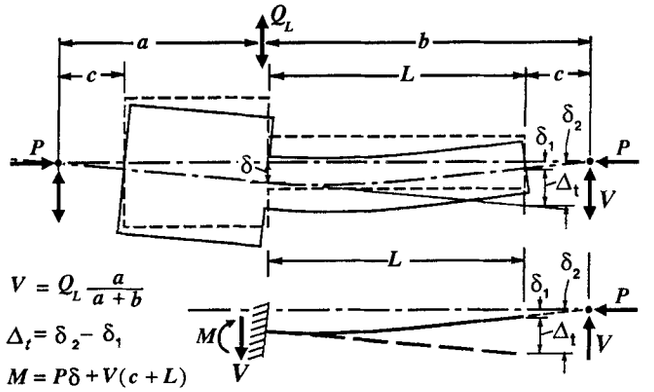

FIG. 6. Idealization of Specimens

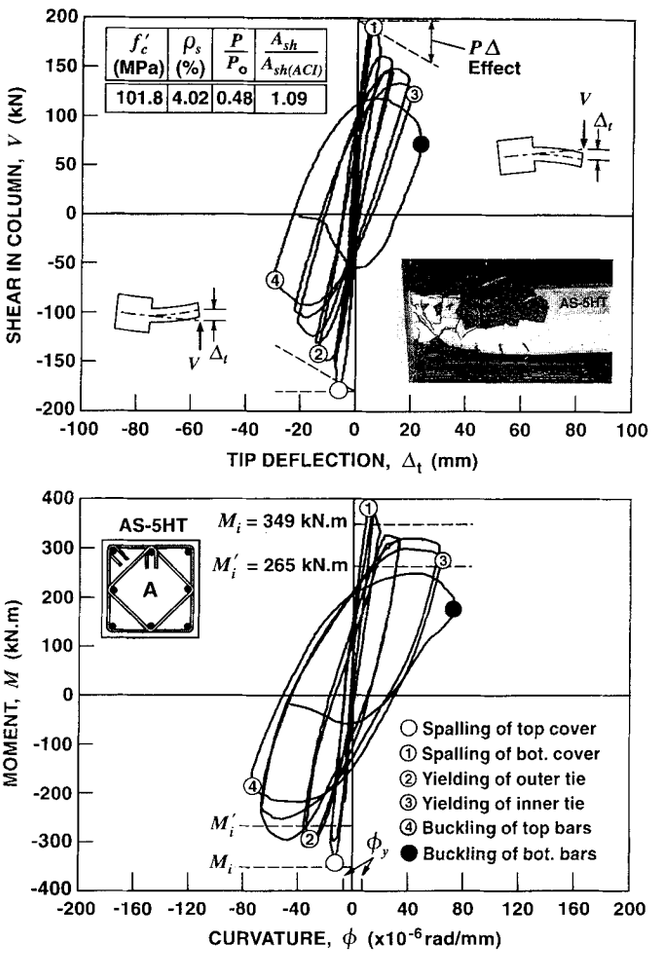

FIG. 7. Behavior of Specimen AS-5HT

cover extended from close to the stub for a distance that ranged between about 350 and 600 mm in different specimens.

In all of the specimens, during the last cycles, buckling of longitudinal bars was observed after yielding of diamond-shaped inner ties and perimeter ties, which was an indication of the commencement of failure. The initiation of buckling of longitudinal bars was determined by visual inspection during each test. At this point, maximum concrete compressive strain in the core at the level of longitudinal reinforcement was 0.010, 0.012, 0.009, and 0.008 for Specimens AS-5HT, AS-6HT, AS-7HT, and ES-8HT, respectively. The maximum concrete compressive strain in the core just before the failure was 0.016, 0.019, 0.011, and 0.012 for Specimens AS-5HT, AS-6HT, AS-7HT, and ES-8HT, respectively. In each test specimen, the failure was accompanied by buckling of the longitudinal bars after the yielding of both inner and perimeter ties. A tie spacing-to-longitudinal bar diameter ratio of 6 was recommended as the design limit by Mander et al. (1988a,b) to avoid premature longitudinal bar buckling. Mau and El-Mabsout (1989) reported that, for cases where the tie spacing-to-bar diameter ratio is smaller than or equal to 6, the stress-strain behavior of the steel was identical in tension and compression. For the specimens reported herein, the tie spacing-to-longitudinal bar diameter ratio ranged between 3.5 and 4.5, and hence premature buckling of the longitudinal bars was not a problem. However, at very large inelastic curvatures it is impossible to prevent buckling of the longitudinal bars, a conclusion similar to that drawn by Scribner (1986).

ANALYSIS OF RESULTS

Because the behavior of reinforced concrete sections and members is not elastic-perfectly plastic, several definitions for ductility and deformability are available in the literature. In this study the ductility parameters suggested by Sheikh and Khoury (1993) are used to evaluate the performance of the specimens, which makes the comparison of the current test results to previous test results (Sheikh and Khoury 1993; Sheikh et al. 1994; Bayrak and Sheikh 1996) more rational. Fig. 5 illustrates these ductility parameters. The definitions for most of the ductility parameters illustrated in Fig. 5 are self explanatory; others however need further explanation. N_Δ and N_ϕ are cumulative displacement and curvature ductility ratios, respectively. These ratios can be used to assess the cumulative amount of inelastic deformations, normalized with respect to yield deformations, experienced by a section or a member. W and E are work damage and energy damage indicators, re-

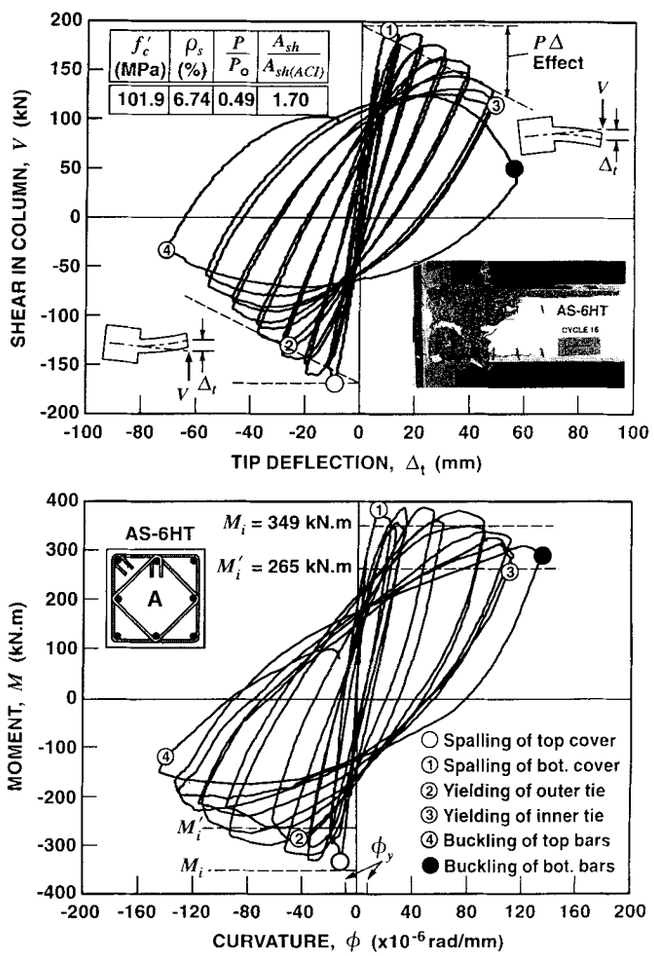

FIG. 8. Behavior of Specimen AS-6HT

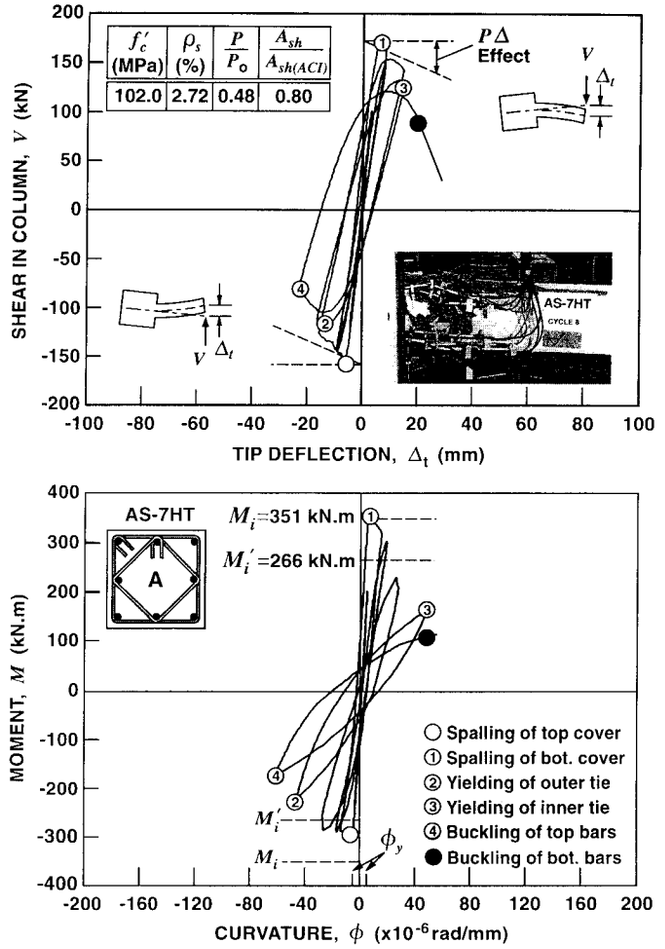

FIG. 9. Behavior of Specimen AS-7HT

spectively. By using these two parameters energy absorption and dissipation characteristics of the test specimens were evaluated. These four parameters can be defined up to the end of a test (in this case subscript t is used in Table 1) or up to the cycle in which the strength loss is ≤20% (in this case subscript 80 is used in Table 1). The moment plotted in the moment-curvature diagram included in Fig. 5 includes the secondary moments, and hence the reduction of M_{max} to 80 or 90% is due to section strength degradation. In the equations presented in Fig. 5 L_f is the length of the extensively damaged region, and h is the height of the column section.

A general study of Figs. 7–10 indicates that UHSC columns having concrete strengths around 102 MPa can be made to behave in a ductile manner under high levels of axial load, provided that a sufficient amount of confining reinforcement is used in an efficient configuration. AS-6HT, which had 70% more reinforcement than the ACI 318-95 requirements, behaved in a very ductile manner, showing a curvature ductility factor $\mu_{\phi 80}$ of 14.0 and a displacement ductility factor μ_Δ of 6.3. The noticeable differences between the responses of the test specimens (Figs. 7–10) indicate that confinement is affected greatly by different variables. It should be recognized that sectional behavior represented by the M-ϕ relationship is of primary concern here because the deformations concentrate at the plastic hinge once the column is loaded in the postelastic range. Further lateral displacements will take place mainly as a result of plastic hinge rotation.

Effect of Concrete Strength

To evaluate the influence of concrete strength on column behavior, Specimen AS-5HT can be compared to Specimen AS-3HT, AS-6HT can be compared to AS-2HT, and ES-8HT to ES-1HT (Figs. 7, 8, and 10–13). Specimens ES-1HT, AS-2HT, and AS-3HT were tested in an earlier stage of the ongoing experimental research program (Bayrak and Sheikh 1996). Details of these test specimens along with Specimen AS-4HT are given in Table 1. The variable $R_{A/P}$ used in Table 1 was defined by Bayrak (1995) as follows:

$$R_{A/P} = \frac{A_{sh}/A_{sh(ACI)}}{P/P_0} \tag{1}$$

It is believed that specimens having the same $R_{A/P}$ ratios and the same type of lateral reinforcement configuration should behave in a similar manner. In the expression for $R_{A/P}$ the level of axial load is presented by the index variable P/P_0 rather than P/f'_cA_g. For columns with similar f'_c, both of these indices provide a similar comparison; whereas for diferent f'_c values in columns the comparison may not remain valid with index P/f'_cA_g. The required amount of lateral reinforcement was observed to be proportional to the strength of concrete for a certain column performance if the axial load is measured as a fraction of P_0 rather than f'_cA_g (Sheikh et al. 1994).

Specimens AS-5HT and AS-3HT were tested under very similar levels of axial load (P/P_0 = 0.48 and 0.50, respectively) and they satisfied the ACI 318-95 requirements for the amount of confinement reinforcement approximately to the same degree ($A_{sh}/A_{sh(ACI)}$ = 1.09 and 1.19, respectively). As a result, the $R_{A/P}$ ratios are very similar in these two specimens. Both the sectional and member performances of these two specimens are very similar (Figs. 7 and 13; Table 1). To conclude this discussion, the comparison of behavior of Specimen AS-6HT to that of Specimen AS-2HT is of great significance. Un-

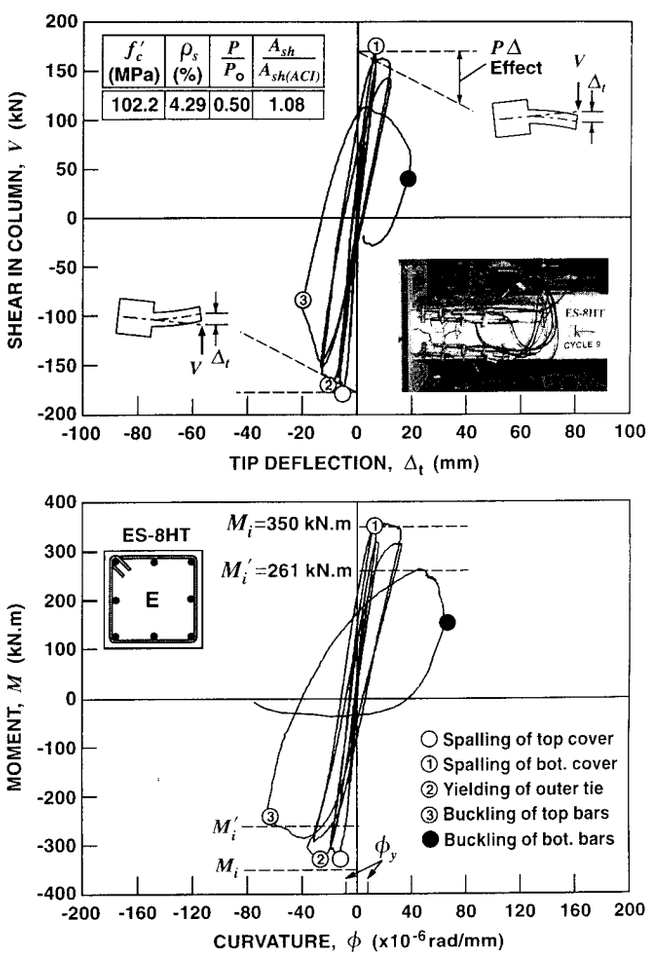

FIG. 10. Behavior of Specimen ES-8HT

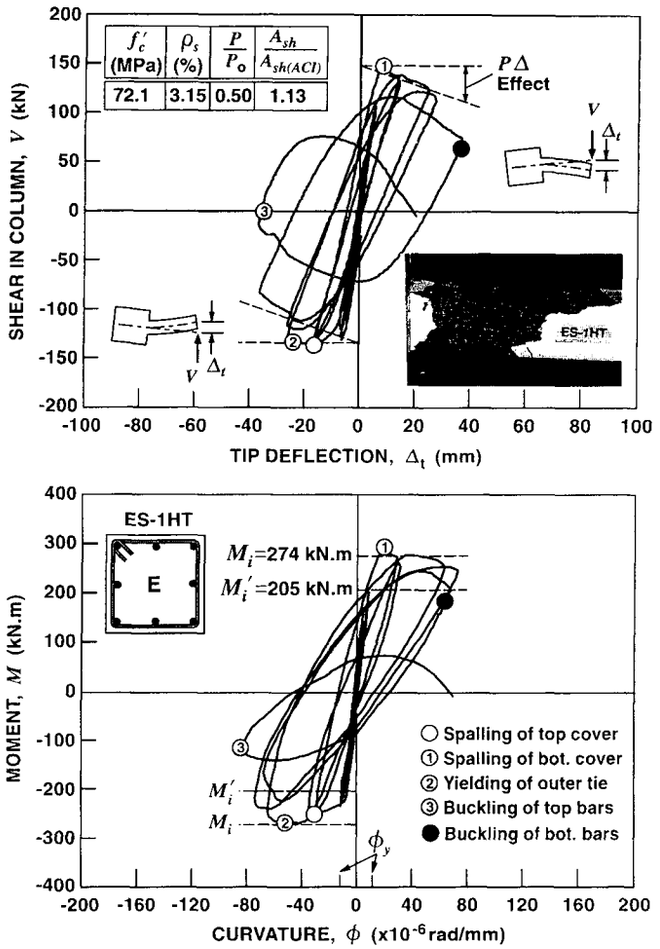

FIG. 11. Behavior of Specimen ES-1HT

like Specimens AS-3HT and AS-5HT that were tested under similar levels of axial load and obeyed the code's requirements for confinement reinforcement to the same degree, Specimens AS-6HT and AS-2HT were tested under different levels of axial load and contained different amounts of lateral reinforcement as indicated by $A_{sh}/A_{sh(ACI)}$. Specimen AS-2HT was tested under a moderate axial load level ($P/P_0 = 0.36$) and had 19% more reinforcement than the code's requirements. Specimen AS-6HT, on the other hand, was tested under a higher level of axial load ($P/P_0 = 0.49$) and contained 70% more reinforcement than the ACI 318-95 requirements for confinement reinforcement. As a result the $R_{A/P}$ ratios are very similar in these two specimens. An examination of the moment-curvature behavior of these two specimens (Figs. 8 and 12) and a comparison of ductility parameters in Table 1 indicate that despite the differences in their concrete strength, these specimens displayed a very similar behavior. An examination of member and section ductility parameters for these specimens (Table 1) indicates that the higher strength concrete specimens have lower deformability, energy absorption, and dissipation capacities initially, but during the latter part of the displacement excursions, these properties improve rapidly and the total values are comparable to those of lower strength concrete specimens. Comparison of sectional and member behavior of Specimens ES-1HT and ES-8HT (Figs. 10 and 11; Table 1) yields to the same conclusion.

Effect of Reinforcement Configuration

The effect of reinforcement configuration on the cycle behavior of UHSC columns can be evaluated by comparing the behavior of Specimens AS-5HT and ES-8HT. Both of these specimens contained 8–9% more reinforcement than the ACI 318-95 code's requirements and were tested under very similar axial load levels. It can be observed from Figs. 7 and 10 that AS-5HT having an $N_{\phi 80}$ value of 27 and an $N_{\phi t}$ value of 49 behaved in a considerably more ductile manner than ES-8HT ($N_{\phi 80} = 14$, $N_{\phi t} = 22$). Furthermore, the curvature ductility factor $\mu_{\phi 80}$ of AS-5HT is 43% larger than that of ES-8HT. Similar comparisons can be made using all of the member and section ductility parameters listed in Table 1; however, the most important evidence that shows weaker behavior of Specimen ES-8HT is its poor energy absorption and dissipation capacity. The energy dissipated in Specimen AS-5HT, measured by the energy damage indicator E_{80}, is 4.4 times as much as the energy dissipated in ES-8HT. Better distribution of reinforcement and better lateral support to the longitudinal bars provided tougher response of UHSC columns, an effect similar to the ones observed for NSC and HSC columns. At this point it should be recognized that the current ACI code's (1995) requirements for the design of confinement reinforcement do not relate the amount of lateral reinforcement to reinforcement configuration. The use of configurations A and E is allowed without any differentiation between the efficiency of confinement in each configuration.

Effect of Amount of Lateral Reinforcement

Specimens AS-5HT and AS-6HT can be compared to evaluate the effect of the amount of lateral reinforcement on the behavior of UHSC columns. An increase in the amount of lateral reinforcement significantly improved the cyclic behavior of the specimen (Figs. 8 and 9). An increase of 67% in the volumetric ratio of tie reinforcement-to-concrete core resulted

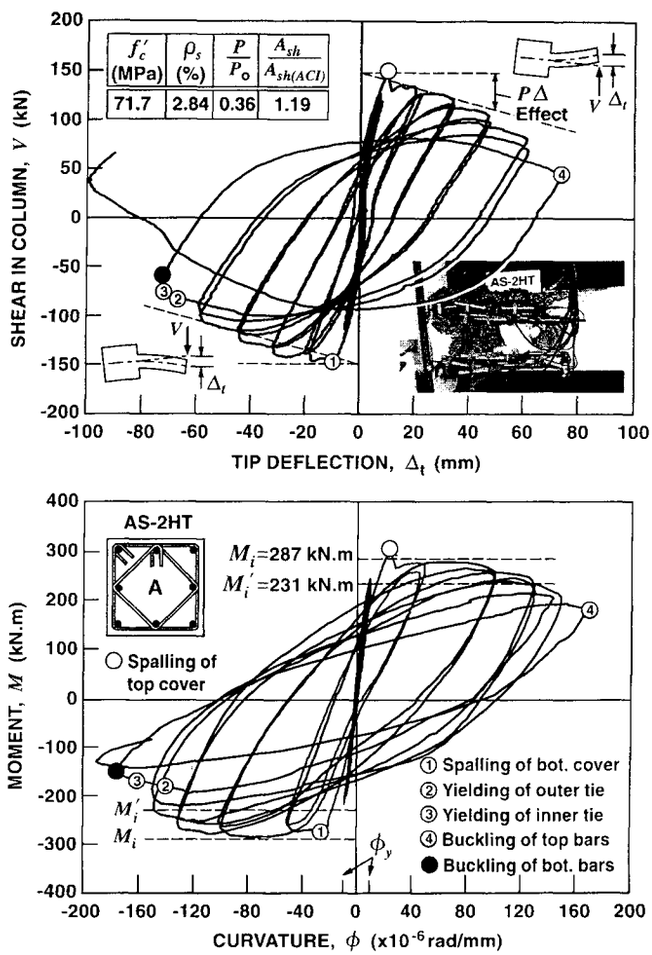

FIG. 12. Behavior of Specimen AS-2HT

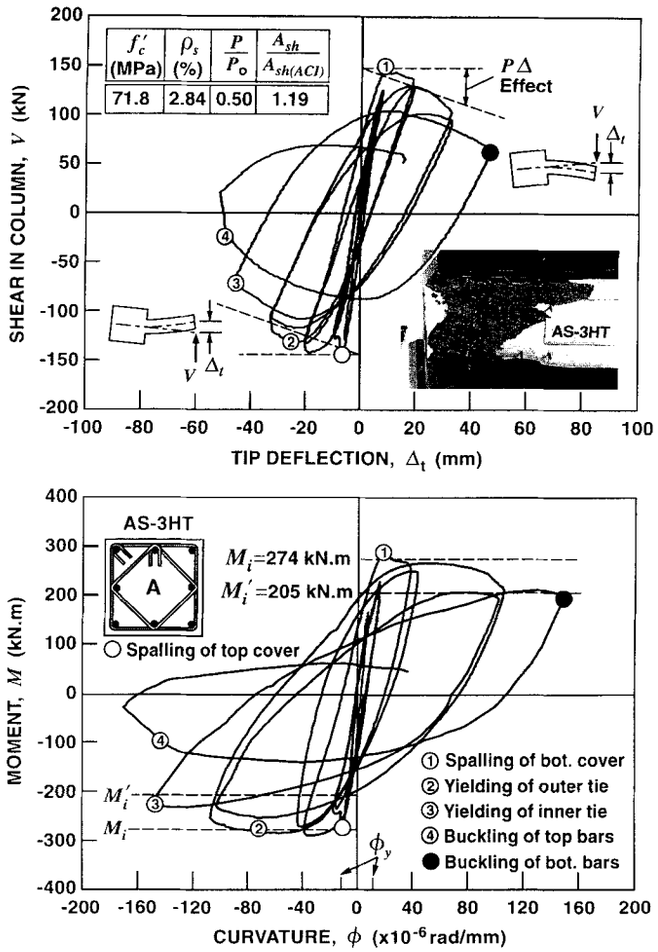

FIG. 13. Behavior of Specimen AS-3HT

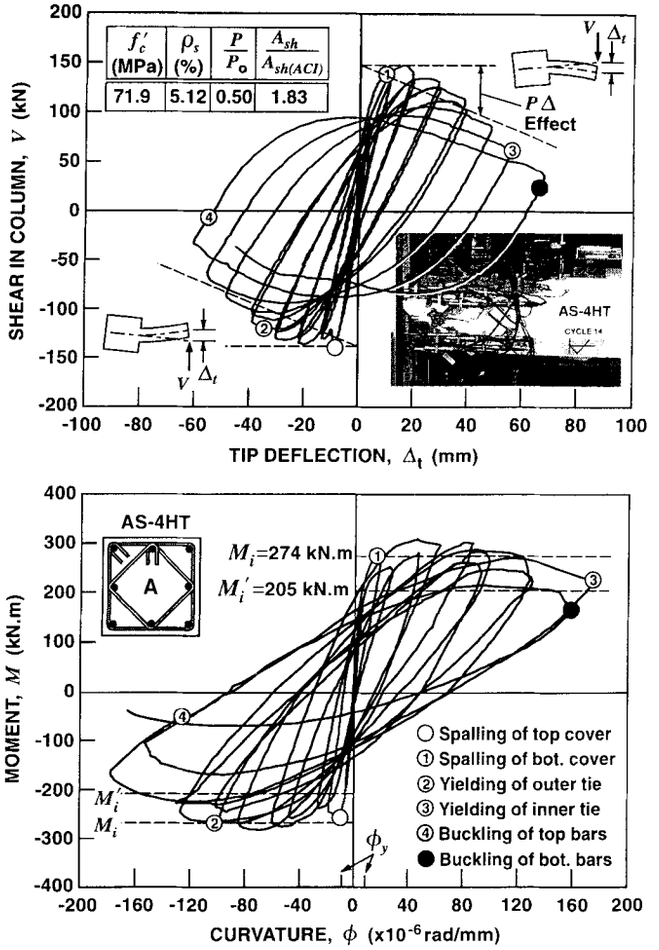

FIG. 14. Behavior of Specimen AS-4HT

in pronounced improvements of energy dissipation capacity, deformability, and ductility (Table 1, Specimens AS-5HT and AS-6HT). Both the stiffness degradation and strength reduction rate with every displacement cycle were lower for AS-6HT compared to AS-5HT.

Specimens AS-3HT and AS-4HT can be compared to evaluate the effect of the amount of lateral reinforcement on the behavior of HSC columns. Volumetric ratio of tie reinforcement-to-concrete core ρ_s for AS-4HT is 80% greater than that of AS-3HT. An increase in the amount of lateral reinforcement significantly improved the behavior of the specimen (Table 1, Specimens AS-3HT and AS-4HT). The section moment capacity was still increasing after the spalling of cover concrete in Specimen AS-4HT, an indication of the excellent confinement of concrete core. It is important to recognize that the observations made for HSC and UHSC columns are similar to those that were made for both NSC columns (Sheikh and Khoury 1993).

Stub Effect

Although the maximum moment occurred at the column-stub interface in all the test specimens, damage initiated away from this section. It seemed that the strength of the section at the column-stub connection was higher than that of the failed section because of the additional confinement provided by the stub. The additional confinement provided by the stub caused a delay in the spreading of cracks in concrete and reduced the tendency of lateral expansion. As a result, the moment capacity of the critical section increased and failure

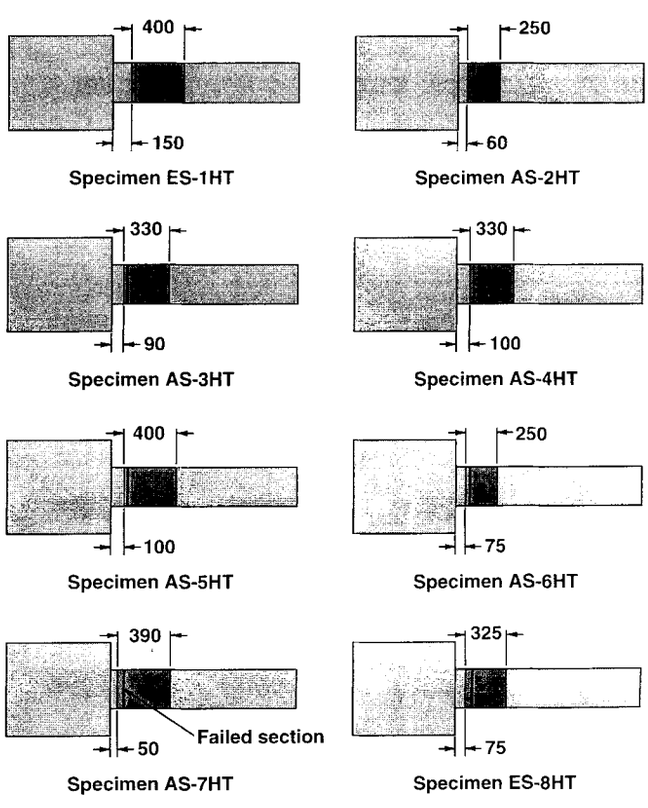

FIG. 15. Extensively Damaged Regions of Test Specimens

shifted to a nearby section. Fig. 15 shows the most damaged regions of the columns in all of the specimens.

Experimental moment capacities M_{exp} of the most critical sections in the extensively damaged regions are presented in Table 2. M_i is the theoretical moment capacity calculated using the HSC stress-strain relationship (Collins and Mitchell 1991) and actual steel properties. M_{ACI} is the moment capacity calculated using the ACI code's (1995) provisions for stress block and actual steel properties. It was observed during testing that cover concrete spalled off suddenly in most of the specimens and that the concrete strain at the time of spalling of the top cover was in the range of 2.4×10^{-3}–3.0×10^{-3}. To evaluate the effect of confinement after the spalling of the cover, M_i and M_{ACI} values are calculated both in the presence and in the absence of the top cover. The M_{exp} values with intact top concrete cover generally represent the unconfined section capacities. Before spalling of the cover, M_{exp} values are very similar to M_i values. M_{ACI} values, however, are significantly higher (10–29%) than the experimental capacities. After the spalling of the cover, M_{exp} values represent the confined section capacities, and they are 11–45% higher than the M_i' values without a top cover.

Fig. 16 illustrates an idealization made for a qualitative evaluation of the stub effect on the moment capacity of the adjacent column section, and moment capacity envelope diagrams. Ignoring the effects of confinement as well as stub, the moment capacity of the unconfined concrete section without a top concrete cover may be assumed to be equal to the theoretical capacity M_i'. Due to confinement, the section moment capacity would increase to $M_{cc} = (1 + C)M_i'$, where C is the confinement effect factor due to ties. The additional enhancement in moment capacity SM_i' due to stub would vary from zero to maximum at the stub's face as suggested by Khoury and Sheikh (1991). Therefore S is the additional confinement effect factor due to stubs (Fig. 16). At this point it should be recognized that the method used to evaluate S and C is not a precise analysis technique. It is rather, a technique used to evaluate and compare relative magnitudes of the confining effects arising from two different sources, i.e., the lateral reinforcement and the stub.

It may be assumed that the failure is approximately initiated at a distance $L_a + L_b$ from the stub, where the stub effect diminishes (Section b-b in Fig. 16). It may also be assumed that the additional restraint provided by the stub may reduce gradually after the failure is initiated and that the zone of failure may extend from Section b-b towards the stub with an extensive damage zone concentrated between Sections a-a and b-b, as shown in Fig. 16. The distance L_a varied from 50 to 150 mm, and L_b varied between 250 and 400 mm in HSC and UHSC specimens (Fig. 15).

The degree of enhancement in section moment capacities of

TABLE 2. Moment Capacities of Specimens

Specimen (1)	Top Concrete Cover in Place: M_i (kN·m) (2)	M_{ACI} (kN·m) (3)	M_{exp} (kN·m) (4)	Top Concrete Cover Spalled Off: M_i' (kN·m) (5)	M_{ACI} (kN·m) (6)	M_{exp} (kN·m) (7)	M_s^a (kN·m) (8)
AS-5HT	349	419	367	265	322	318	402
AS-6HT	349	416	361	262	316	356	396
AS-7HT	351	419	326	266	323	296	359
ES-8HT	350	416	342	261	315	321	377
ES-1HT	274	310	272	205	237	274	309
AS-2HT	287	314	286	231	260	282	323
AS-3HT	274	310	279	205	238	274	320
AS-4HT	274	310	266	204	237	296	324

[a]Maximum experimental moment at section adjacent to stub as an average of both load directions.

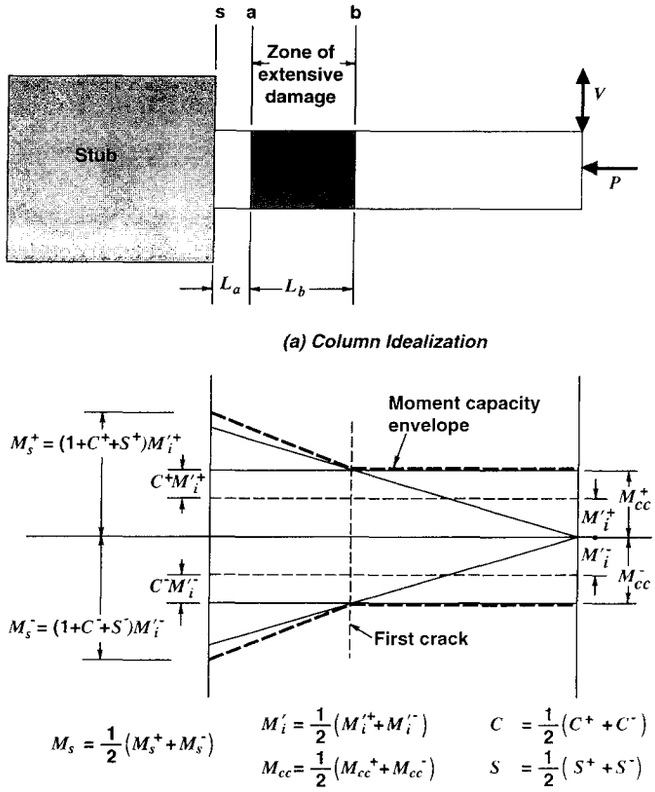

FIG. 16. Quantitative Evaluation of Stub Effect

TABLE 3. Degree of Enhancement in Moment Capacities

Specimen (1)	Moment Enhancement Ratios: M_a/M_i' (2)	M_a/M_i' (3)	M_b/M_i' (4)	Confinement Effect Factor: C (5)	Stub Effect Factor: S (6)	$C + S$ (7)
AS-5HT	1.517	1.411	1.189	0.189	0.328	0.517
AS-6HT	1.511	1.444	1.306	0.306	0.205	0.511
AS-7HT	1.350	1.309	1.067	0.067	0.283	0.350
ES-8HT	1.444	1.380	1.190	0.190	0.254	0.444
ES-1HT	1.507	1.380	1.180	0.180	0.327	0.507
AS-2HT	1.398	1.348	1.208	0.208	0.190	0.398
AS-3HT	1.561	1.481	1.282	0.282	0.279	0.561
AS-4HT	1.588	1.506	1.304	0.304	0.284	0.588
Average	1.485	1.407	1.206	0.216	0.269	0.485

the tested specimens is analyzed and the results are presented in Table 3. Enhancement in the moment capacity due to confinement is in the range of 7–31% of the theoretical moment capacity M_i'. Stub restraint increased the capacity further by at least 19–33%. The maximum moment experienced by the columns at the column-stub interface ranged from 1.35 to 1.59 times the theoretical capacity M_i'. This moment did not cause failure in any of the specimens. It should be noted that for this analysis Section b-b (Fig. 16) was considered to be the section where failure initiated, and the effect of stub restraint was minimal. Furthermore, Specimens AS-2HT and AS-3HT were analyzed using a plasticity-based finite-element analysis technique. This analysis was performed using ABAQUS (*ABAQUS* 1992), and the material model was coded as user-defined subroutine. Predictions for L_a and L_b were 98 and 103% of the values shown in Fig. 15 and predictions C and S were in reasonable agreement with the values listed in Table 3. Further discussion about this part of the work is omitted due to space

TABLE 4. Comparison of Predicted and Observed Curvature Ductility Factors

Specimen (1)	Properties			Curvature Ductility Factors, $\mu_{\phi 80}$				
	f'_c (MPa) (2)	$\frac{A_{sh}}{A_{sh(ACI)}}$ (3)	$\frac{P}{P_0}$ (4)	Observed $\mu_{\phi 80EXP}$ (5)	Prediction by HSC formulation, $\mu_{\phi 80HSC}$ (6)	$\frac{\mu_{\phi 80HSC}}{\mu_{\phi 80EXP}}$ (7)	Prediction by NSC formulation, $\mu_{\phi 80NSC}$ (8)	$\frac{\mu_{\phi 80NSC}}{\mu_{\phi 80EXP}}$ (9)
AS-5HT	101.8	1.09	0.48	9.6	10.1	1.05	15.7	1.64
AS-6HT	101.9	1.70	0.49	14.0	16.8	1.20	22.6	1.61
AS-7HT	102.0	0.80	0.48	7.2	6.9	0.96	12.0	1.67
ES-8HT	102.2	1.08	0.50	6.7	6.7	1.00	6.7	1.00
ES-1HT	72.1	1.13	0.50	6.6	6.6	1.00	7.0	1.06
AS-2HT	71.7	1.19	0.36	15.8	14.5	0.92	20.4	1.29
AS-3HT	71.8	1.19	0.50	10.1	10.5	1.04	16.2	1.60
AS-4HT	71.9	1.83	0.50	21.2	17.7	0.83	23.5	1.11
Average	—	—	—	11.4	11.2	1.00	15.5	1.37

limitations and is beyond the scope of this paper. However, it should be appreciated that this technique was used to evaluate the stub effect of the specimens tested in this study and may not provide accurate results for other specimens.

Effect of Axial Load

Effect of axial load is evaluated using HSC columns. Specimens AS-2HT and AS-3HT (Figs. 12 and 13) were identical, containing the same amount of lateral reinforcement that was 19% more than the ACI code's (1995) requirements. Specimen AS-2HT was tested under a moderate level of axial load ($P/P_0 = 0.36$); whereas AS-3HT was tested under a higher axial load level ($P/P_0 = 0.50$). Hence, the axial load level is the only variable for the comparative analysis of these two HSC specimens. An increase in axial load caused substantial reductions in the curvature ductility factors, $\mu_{\phi 80}$ and $\mu_{\phi 90}$. Moreover, the cumulative curvature ductility ratios showed significant reductions, from 53 to 20 for $N_{\phi 80}$ and 113 to 42 for $N_{\phi t}$, as a result of increased load. Similar conclusions can be drawn from the comparison of the energy damage indicators, E_{80} and E_4; in fact, energy damage indicators appear to be affected the most compared to the other parameters. The energy dissipated in Specimen AS-2HT measured by E_{80} and E_t is 3.6–4 times as much as the energy dissipated in Specimen AS-3HT. Reductions of 19, 54, and 67% were observed in displacement ductility factor μ_Δ, cumulative displacement ductility ratio $N_{\Delta t}$, and work damage indicator W_t, respectively, due to the increase in axial load. A higher axial load resulted in an increase in the rate of stiffness degradation with every load cycle and adversely affected the cyclic performance of HSC columns (Bayrak and Sheikh 1996). These results underlined the need to incorporate the level of axial load in computing the required amount of confining reinforcement.

CONFINEMENT REINFORCEMENT REQUIREMENTS FOR HSC COLUMNS

Sheikh and Khoury (1997) proposed a procedure for the design of confinement reinforcement, for a given ductile performance that takes into account parameters such as reinforcement distribution and axial load level. This method is suggested for the design of columns that have concrete strengths up to 55 MPa. Accuracy of this procedure is checked against the results from this experimental program. It is found that the average of all eight predictions made by the design equations suggested by Sheikh and Khoury (1997) (for Specimens ES-1HT, AS-2HT, AS-3HT, AS-4HT, AS-5HT, AS-6HT, AS-7HT, and ES-8HT) is 37% larger than the average experimental values (Table 4). Standard deviation from the mean was 29% for the HSC and UHSC specimens. To improve the predictions, a regression analysis was performed using results from Specimens ES-1HT, AS-2HT, AS-3HT, AS-4HT, AS-5HT, AS-6HT, AS-7HT, and ES-8HT. As suggested by Sheikh and Khoury (1997) the required amount of lateral reinforcement in tied columns was assumed to be

$$A_{sh} = [A_{sh(ACI)}] \cdot \alpha \cdot Y_P \cdot Y_\phi \tag{2}$$

where $\Delta_{sh(ACI)}$ = total cross-sectional area of rectilinear ties as suggested by the ACI 318-95 code; α = configuration efficiency factor [$\alpha = 1$ when all longitudinal bars are laterally supported by tie bends, $\alpha > 1$ when some of the longitudinal bars are not supported by tie bends, e.g., for NSC columns having E-type reinforcement configuration α was suggested to be 2.5 (Sheikh and Khoury 1997)]; Y_P = parameter to take into account the effect of axial load; and Y_ϕ = parameter to take into account section ductility demand.

The expressions suggested for Y_P and Y_ϕ are kept in the same form as the original model as follows:

$$Y_P = a_1 + a_2 \cdot \left(\frac{P}{P_0}\right) a_3 \tag{3}$$

$$Y_\phi = a_4 \cdot (\mu_{\phi 80}) a_5 \tag{4}$$

where a_1 to a_5 = constants that were evaluated performing a regression analysis using results from test series in which f'_c ranged from 30 to 55 MPa.

In the application to specimens having concrete strengths varying between 72 and 102 MPa, it was found that constants a_1, a_2, and a_3 remained the same and constants a_4 and a_5 changed. In other words, the effect of axial load on the lateral reinforcement demand is not influenced significantly by concrete strength. Section ductility demand measured by $\mu_{\phi 80}$, on the other hand, is influenced by concrete strength. This is because higher strength concrete specimens have lower deformability and energy absorption capacities initially. These properties improve considerably during the latter part of the displacement excursions as discussed previously. Curvature ductility factor $\mu_{\phi 80}$ does not reflect the total behavior of a column section. Instead, it focuses only upon the part of a moment-curvature relationship in which the strength loss is smaller than or equal to 20% of the maximum bending moment. For NSC columns a_4 and a_5 were found to be equal to 1/29 and 1.15, respectively. Using the results of four HSC specimens and four UHSC specimens a least-squares analysis yielded in $a_4 = 1/8.12$ and $a_5 = 0.82$. With these new constants, the average of the predicted curvature ductility ratios is roughly equal to the average of the experimental values, and the standard deviation from the mean is 10%. Furthermore, the value of configuration efficiency factor α for E-type HSC and UHSC columns is calculated to be equal to 1.35. At this point it should be recognized that regression analysis for a_4 and a_5 were performed only on eight columns having concrete strengths ranging from 72 to 102 MPa. Constants determined in this study by regression analysis may be refined with the availability of more experimental data, but it is believed that

the general form of the equation would remain unchanged. Regression analyses for a_1, a_2, and a_3 were performed on 17 columns having concrete strengths ranging from 30 to 102 MPa. The following equation summarizes the suggested design procedure for the design of confinement reinforcement for HSC columns with f'_c in the range of 55 MPa to over 100 MPa:

$$A_{sh} = [A_{sh(ACI)}] \cdot \alpha \cdot \left[1 + 13 \cdot \left(\frac{P}{P_0}\right)^5\right] \cdot \left[\frac{(\mu_{\phi 80})^{0.82}}{8.12}\right] \quad (5)$$

As a first impression (5) may look complicated to a design practitioner, but it requires little extra effort than using the ACI code equation. The designer would generally know the level of axial load measured by P/P_0 for the column under consideration and should be able to assess the curvature ductility factor needed, e.g., based on the response reduction or the modification factor used in the calculation of the design forces. Factor α, on the other hand, can be taken as unity for columns in which a minimum of three longitudinal bars are effectively supported by tie corners on each face of the column and hooks are anchored into the core concrete (Sheikh and Khoury 1997). It is recommended that for HSC and UHSC columns that need to exhibit highly ductile performance, configurations that will produce $\alpha = 1$ should be used.

To compare the suggested design procedure to the existing design codes, confinement reinforcement design for a 500 × 500 mm column is shown in Fig. 17. The concrete strength is taken to be equal to 90 MPa; the yield strength of both longitudinal and lateral reinforcement is taken to be equal to 450 MPa. An A-type reinforcement configuration that provides excellent lateral support to longitudinal bars by the tie bends is used for this particular column. Spacing of tie sets is selected to be equal to 100 mm. The area of confinement reinforcement required by the ACI 318-95 code, the NZS 3101:1995 code, and the suggested design procedure are calculated. The results are normalized with respect to ACI code's requirements. At this point it should be recognized that the ACI 318-95 provisions for confinement reinforcement results in a constant reinforcement area for different levels of axial load and different section performance as indicated by the curvature ductility factor $\mu_{\phi 80}$.

It can be observed from Fig. 17, that the column designed according to ACI 318-95 code's provisions is able to supply a curvature ductility factor of ~8 if the axial load on this column is $0.5P_0$. It is stated in the NZS 3101:1995 code that the aim is to obtain a curvature ductility factor of at least 10. Sheikh and Khoury (1993) suggested that columns that are able to supply a curvature ductility factor of at least 16 can be considered as highly ductile columns. At this point it should be understood that the ductility factor used in the New Zealand code uses a secant approach to determine the yield curvature, whereas in the study conducted by Sheikh and Khoury (1993) a different approach is used to calculate the yield curvature. A curvature ductility factor of 10 calculated using NZS 3101:1995 definitions is approximately equivalent to a curvature ductility factor of 16–20 calculated using the definitions presented in Fig. 5. If the confinement reinforcement in the sample HSC column under consideration were designed according to ACI provisions, it would not be able to provide a curvature ductility factor of 16 for small P/P_0 values. Hence, columns designed according to the current ACI code can display a wide range of behaviors from very ductile to brittle, depending on the level of axial load and the efficiency of the reinforcement configuration.

All of the eight columns used in this study were tested under moderate to high axial load levels. Therefore it is believed that the equation suggested here should be checked against data from columns tested under lower axial load levels. However,

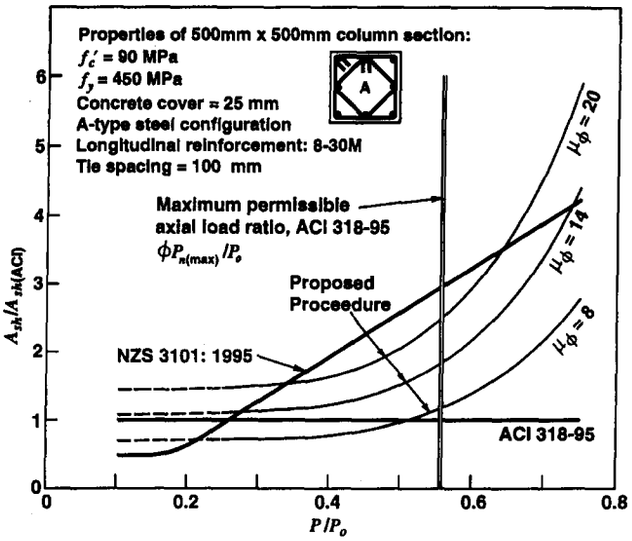

FIG. 17. Confinement Reinforcement Requirements for HSC Columns (f'_c > 55 MPa)

it is obvious that the behavior of compressed concrete would improve significantly if it is confined properly regardless of the level of axial load. Fig. 17 shows that even for axial load levels around $0.2_x(P/P_0)$, the required amount of lateral reinforcement is larger than that required by the ACI code, if highly ductile performance is needed.

CONCLUDING REMARKS

Four UHSC column-stub specimens made of 102-MPa concrete were tested under high axial load levels and reversed cyclic lateral displacement excursions. Results from earlier tests on four similar HSC specimens made of 72-MPa concrete are also included and used in evaluating the effect of concrete strength on the response of tied columns. The following conclusions can be drawn from the current research reported in this paper:

- UHSC columns that are made with 102-MPa concrete can be made to behave in a ductile manner under high levels of axial load, provided that a sufficient amount of lateral reinforcement is used in an efficient configuration. A UHSC column specimen made with 102-MPa concrete and having 70% more reinforcement than the code's requirements displayed a very ductile behavior showing a curvature ductility factor of 14.0 and a displacement ductility factor of 6.3. As in NSC and HSC specimens, behavior of UHSC columns subjected to constant axial load and reversed cyclic lateral load is substantially influenced by the confinement provided by rectilinear ties.
- An increase in axial load reduces the column's deformability and ductility and accelerates strength and stiffness degradation with every load cycle. To compensate for this effect a larger amount of lateral reinforcement is required. Therefore, the axial load level should be incorporated as a design parameter in the design of confinement reinforcement.
- An examination of member and section ductility parameters for comparable specimens indicates that the higher strength concrete specimens have lower deformability and energy absorption and dissipation capacities initially, but during the latter part of the displacement excursions, these properties improve rapidly and the total values are comparable to those of lower strength concrete specimens.
- UHSC columns having E-type reinforcement configuration (middle longitudinal bars are not supported by tie

bends) have lower energy dissipation and deformation capacities than those having A-type reinforcement configuration (all eight longitudinal bars are supported by tie bends). Better distribution of reinforcement and better lateral support to the longitudinal bars provided tougher response of UHSC columns, an effect similar to the ones observed for NSC and HSC columns. ACI code's (1995) requirements for the design of confinement reinforcement do not relate the amount of lateral reinforcement to reinforcement configuration and the level of axial load. However, current experimental results suggest that reinforcement configuration and axial load level must be considered in the design of confinement reinforcement.

ACKNOWLEDGMENTS

The research for this study was supported by grants from the Natural Sciences and Engineering Council of Canada. The experimental work was performed in the Structural Testing Laboratories of the University of Toronto, Toronto, Ontario, Canada.

APPENDIX. REFERENCES

ABAQUS User's Manual Version 5.2. (1992). Hibbit, Karlsson & Sorensen Inc.

Bayrak, O. (1995). "High strength concrete columns subjected to earthquake type loading," MASc thesis, Dept. of Civ. Engrg., Univ. of Toronto, Toronto, Ont., Canada, 239.

Bayrak, O., and Sheikh, S. A. (1996). "Confinement steel requirements for high strength concrete columns." *Proc., 11th World Conf. on Earthquake Engrg.*, 8.

"Building code requirements for reinforced concrete and commentary." (1995). *ACI 318-95/ACI 381R-95*, Am. Concrete Inst., Detroit, Mich., 369.

"Code for design of concrete structures for building." (1994). *CAN3-A23.3-M94*, Can. Standards Assn., Rexdale, Ont., Canada, 199.

"Code of practice for the design of concrete structures." (1995a). Part 1: The design of concrete structures, *NZS 3101:1995*, New Zealand Standards, Wellington, New Zealand, 256.

"Code of practice for the design of concrete structures." (1995b). Part II: Commentary on the design of concrete structures, *NZS 3101:1995*, New Zealand Standards, Wellington, New Zealand, 264.

Collins, M. P., and Mitchell, D. (1991). *Prestressed concrete structures*. Prentice-Hall, Inc., Englewood Cliffs, N.J., 766.

Khoury, S. S., and Sheikh, S. A. (1991). "Behavior of normal and high strength confined concrete columns with and without stubs." *Res. Rep. No. UHCEE 91-4*, Dept. of Civ. and Envir. Engrg., Univ. of Houston, Tex., 345.

Mander, J. B., Priestley, M. J. N., and Park, R. (1988a). "Observed stress-strain behavior of confined concrete." *J. Struct. Engrg.*, ASCE, 114(8), 1827–1849.

Mander, J. B., Priestley, M. J. N., and Park, R. (1988b). "Theoretical stress-strain model for confined concrete." *J. Struct. Engrg.*, ASCE, 114(8), 1804–1826.

Mau, S. T., and El-Mabsout, M. (1989). "Inelastic buckling of reinforcing bars." *J. Engrg. Mech.*, ASCE, 115(1), 1–17.

Mitchell, D., and Paultre, P. (1994). "Ductility and overstrength in seismic design of reinforced concrete structures." *Can. J. Civ. Engrg.*, Ottawa, Canada, 21(6), 1049–1060.

Paulay, T. (1977). "Seismic design of ductile moment resisting reinforced concrete frames, columns: Evaluation of actions." *Bull. New Zealand Nat. Soc. for Earthquake Engrg.*, Waikanae, New Zealand, 10(2), 85–94.

Scribner, C. F. (1986). "Reinforcement buckling in reinforced concrete flexural members." *ACI J.*, 83(6), 966–973.

Sheikh, S. A., and Khoury, S. S. (1993). "Confined concrete columns with stubs." *ACI Struct. J.*, 90(4), 414–431.

Sheikh, S. A., and Khoury, S. S. (1997). "A performance-based approach for the design of confining steel in tied columns." *ACI Struct. J.*, 94(4), 421–431.

Sheikh, S. A., Shah, D. V., and Khoury, S. S. (1994). "Confinement of high-strength concrete columns." *ACI Struct. J.*, 91(1), 100–111.

Sheikh, S. A., and Toklucu, M. A. (1993). "Reinforced concrete columns confined by circular spirals and hoops." *ACI Struct. J.*, 90(5), 542–553.

Sheikh, S. A., and Uzumeri, S. M. (1980). "Strength and ductility of tied concrete columns." *J. Struct. Div.*, ASCE, 106(5), 1079–1102.

Watson, S., and Park, R. (1994). "Simulated seismic load tests on reinforced concrete columns." *J. Struct. Engrg.*, ASCE, 120(6), 1825–1849.

Watson, S., Zahn, F. A., and Park, R. (1994). "Confining reinforcement for concrete columns." *J. Struct. Engrg.*, ASCE, 120(6), 1798–1824.